Quantitative Models of Phage-Antibiotic Combination Therapy

Rogelio A. Rodriguez-Gonzalez,a,b Chung Yin Leung,b,c Benjamin K. Chan,d Paul E. Turner,d,e (ID) Joshua S. Weitzb,c

aInterdisciplinary Graduate Program in Quantitative Biosciences, Georgia Institute of Technology, Atlanta, Georgia, USA
bSchool of Biological Sciences, Georgia Institute of Technology, Atlanta, Georgia, USA
cSchool of Physics, Georgia Institute of Technology, Atlanta, Georgia, USA
dDepartment of Ecology and Evolutionary Biology, Yale University, New Haven, Connecticut, USA
eProgram in Microbiology, Yale School of Medicine, New Haven, Connecticut, USA

ABSTRACT The spread of multidrug-resistant (MDR) bacteria is a global public health crisis. Bacteriophage therapy (or "phage therapy") constitutes a potential alternative approach to treat MDR infections. However, the effective use of phage therapy may be limited when phage-resistant bacterial mutants evolve and proliferate during treatment. Here, we develop a nonlinear population dynamics model of combination therapy that accounts for the system-level interactions between bacteria, phage, and antibiotics for *in vivo* application given an immune response against bacteria. We simulate the combination therapy model for two strains of *Pseudomonas aeruginosa*, one which is phage sensitive (and antibiotic resistant) and one which is antibiotic sensitive (and phage resistant). We find that combination therapy outperforms either phage or antibiotic alone and that therapeutic effectiveness is enhanced given interaction with innate immune responses. Notably, therapeutic success can be achieved even at subinhibitory concentrations of antibiotics, e.g., ciprofloxacin. These *in silico* findings provide further support to the nascent application of combination therapy to treat MDR bacterial infections, while highlighting the role of innate immunity in shaping therapeutic outcomes.

IMPORTANCE This work develops and analyzes a novel model of phage-antibiotic combination therapy, specifically adapted to an *in vivo* context. The objective is to explore the underlying basis for clinical application of combination therapy utilizing bacteriophage that target antibiotic efflux pumps in *Pseudomonas aeruginosa*. In doing so, the paper addresses three key questions. How robust is combination therapy to variation in the resistance profiles of pathogens? What is the role of immune responses in shaping therapeutic outcomes? What levels of phage and antibiotics are necessary for curative success? As we show, combination therapy outperforms either phage or antibiotic alone, and therapeutic effectiveness is enhanced given interaction with innate immune responses. Notably, therapeutic success can be achieved even at subinhibitory concentrations of antibiotic. These *in silico* findings provide further support to the nascent application of combination therapy to treat MDR bacterial infections, while highlighting the role of system-level feedbacks in shaping therapeutic outcomes.

KEYWORDS antimicrobial agents, bacteriophage therapy, bacteriophages, evolutionary biology, mathematical modeling, microbial ecology

Multidrug-resistant (MDR) bacterial infections are a threat to global health. The World Health Organization (WHO) has reported that drug-resistant tuberculosis alone kills 250,000 people each year (1). Moreover, the United States Centers for Disease Control and Prevention (CDC) have reported 23,000 deaths each year attributed to drug-resistant pathogens, while their European counterparts have reported 25,000

deaths each year resulting from drug-resistant infections (2, 3). The WHO has identified and prioritized 12 MDR pathogens (1) in order to guide efforts toward the development of new antimicrobial treatments. The Gram-negative bacterium *Pseudomonas aeruginosa* has been identified as a critical priority by the WHO (1).

Bacterial viruses (i.e., bacteriophage or "phage") represent an alternative approach to treat MDR bacterial infections. Phage lysis of bacterial cells can drastically change bacterial population densities. In doing so, phage exert a strong selection pressure on the bacterial population. As a result, phage-resistant mutants can appear and become dominant (4–6), whether via surface-based resistance (4, 7) or intracellular mechanisms (8). The possibility that phage therapy may select for phage-resistant bacterial mutants has increased interest in identifying strategies to combine phage with other therapeutics, e.g., antibiotics (4, 6, 7, 9–11). However, the realized outcomes of combination strategies are varied, ranging from successes *in vitro* (9) and *in vivo* (4, 11) to failure given *in vitro* settings (6).

In many cases, the mechanism(s) underlying potential phage-antibiotic interactions is unknown. There are exceptions; for example, *Escherichia coli* phage TLS and U136B infect the bacterium by attaching to the outer membrane protein TolC, which is part of the AcrAB-TolC efflux system (12, 13). It has been shown that phage TLS selects for *tolC* mutants that are hypersensitive to novobiocin (13). Moreover, TolC has been identified as a phage receptor in other Gram-negative pathogens (14, 15), giving further support to the combined use of phage and antibiotics. Similarly, the phage OMKO1 may be able to use multiple binding targets to infect *P. aeruginosa*, including the type IV pilus and the multidrug efflux pump MexAB/MexXY (7); both mechanisms can result in selection against drug resistance.

The ability of phage OMKO1 to select against drug resistance in *P. aeruginosa* suggests that a combination treatment of *P. aeruginosa* with phage OMKO1 and antibiotics can lead to an evolutionary tradeoff between phage and antibiotic resistance (7, 11). Phage-resistant mutants can show impairments of the multidrug efflux pump MexAB/MexXY (7), such as reduced functionality (or loss) of outer membrane porin M (OprM). This protein is part of the efflux pump complex and may act as a cell receptor of the phage OMKO1. Mutations in the gene encoding OprM can impair phage infection and restore the sensitivity to some classes of antibiotics, including ciprofloxacin (CP) (7). Such an evolutionary tradeoff may be leveraged clinically to limit the spread of resistance to phage and antibiotics. Therapeutic application of phage and antibiotics *in vivo* necessarily involves interactions with a new class of antimicrobial agents: effector cells within the immune system. Recent work has shown that phage and innate immune cells, specifically neutrophils, combine synergistically to clear otherwise fatal respiratory infections which neither phage nor the innate immune response could eliminate alone (5). This "immunophage synergy" is hypothesized to result from density-dependent feedback mechanisms (16). Phage lysis decreases bacterial densities such that the activated immune response can clear bacteria; without phage, the bacterial densities increase to sufficiently high levels that are outside the range of control by immune cells. However, the potential role of the innate immune response in the context of phage-antibiotic combination therapy remains largely unexplored.

Here, we develop and analyze a mathematical model of phage-antibiotic combination therapy that builds on the synergistic interactions between phage, antibiotic, and immune cells. In doing so, we extend a mathematical model of immunophage synergy (16) to take into account the pharmacodynamics and pharmacokinetics of an antibiotic, e.g., ciprofloxacin. At the core of the combination therapy model is its multiple-targeting approach: the phage target phage-sensitive (antibiotic-resistant) bacteria while the antibiotic targets phage-resistant (antibiotic-sensitive) mutants (7, 11). Critically, in this model we assume that immune effector cells can target both bacterial strains. As we show, combination therapy successfully clears infections insofar as immune responses are active. Our proof-of-principle systems-level model highlights the role of immune responses in developing and assessing the effectiveness of phage-

based therapeutics for treatment of MDR pathogens, particularly MDR *P. aeruginosa*, which exhibit evolutionary tradeoffs.

Combination therapy model. We propose a combination therapy model consisting of a system of nonlinear, ordinary differential equations representing the interactions among bacteria, phage, antibiotics, and the innate immune system (see Fig. 1). Two strains of bacteria are included, one of which is phage sensitive (B_P) and the other of which is antibiotic sensitive (B_A). The strains B_P and B_A reproduce given limitation by a carrying capacity. B_P is infected and lysed by phage (P) but resists the antibiotic, while the B_A population is killed by the antibiotic but is resistant to phage (for an *in vitro* model of bacteriophage therapy with fully susceptible and resistant types, see reference 17). We do not consider double-resistant mutants in our model due to the evolutionary tradeoff between resistance against phage and antibiotics observed for *P. aeruginosa* (7). Phage replicate inside the host B_P and decay in the environment. The antibiotic is administered at a constant concentration; then, it is metabolized and removed at a fixed rate. The population dynamics are governed by the following set of equations:

$$\dot{B}_P = \overbrace{r_P B_P \left(1 - \frac{B_{\text{tot}}}{K_C}\right)}^{B_P \text{ growth}} \overbrace{(1 - \mu_1)}^{\text{Mutation to } B_A} + \overbrace{\mu_2 r_A B_A \left(1 - \frac{B_{\text{tot}}}{K_C}\right)}^{\text{Mutation from } B_A}$$

$$- \overbrace{\frac{\varepsilon I B_P}{1 + \frac{B_{\text{tot}}}{K_D}}}^{\text{Immune killing}} - \overbrace{B_P F(P)}^{\text{Lysis}} \tag{1}$$

$$\dot{B}_A = \overbrace{r_A B_A \left(1 - \frac{B_{\text{tot}}}{K_C}\right)}^{B_A \text{ growth}} \overbrace{(1 - \mu_2)}^{\text{Mutation to } B_P} + \overbrace{\mu_1 r_P B_P \left(1 - \frac{B_{\text{tot}}}{K_C}\right)}^{\text{Mutation from } B_P}$$

$$- \overbrace{\frac{\varepsilon I B_A}{1 + \frac{B_{\text{tot}}}{K_D}}}^{\text{Immune killing}} - \overbrace{\kappa_{\text{kill}} \frac{A^H}{\text{EC}_{50}^H + A^H} B_A}^{\text{Antibiotic killing}}, \tag{2}$$

$$\dot{P} = \overbrace{\tilde{\beta} B_P F(P)}^{\text{Viral release}} - \overbrace{\omega P}^{\text{Decay}}, \tag{3}$$

$$\dot{I} = \overbrace{\alpha I \left(1 - \frac{I}{K_I}\right)\left(\frac{B_{\text{tot}}}{B_{\text{tot}} + K_N}\right)}^{\text{Immune stimulation}}, \tag{4}$$

$$\dot{A} = \overbrace{A_I}^{\text{Antibiotic input}} - \overbrace{\theta A}^{\text{Elimination}} \tag{5}$$

In this model, phage-sensitive bacteria grow at a maximum rate r_P, while antibiotic-sensitive bacteria (B_A) grow at a maximum rate r_A. The total bacterial density, $B_{\text{tot}} = B_P + B_A$, is limited by the carrying capacity K_C. Phage infect and lyse B_P bacteria at a rate $F(P)$. Antibiotic killing is approximated by a Hill function with the nonlinear coefficient (H) (18–21). The maximum antibiotic killing rate is κ_{kill}, while EC_{50} is the concentration of the antibiotic, here considered ciprofloxacin, at which the antibiotic effect is half the maximum. Phage P replicate with a burst size $\beta = \tilde{\beta} + 1$ and decay at a rate ω. We assume that antibiotic dynamics are relatively fast and use a quasi-steady-state approximation of $A^* = A_I/\theta$.

When simulating an *in vivo* scenario, the host innate immune response, I, is activated by the presence of bacteria and increases with a maximum rate α. K_N is a half-saturation constant, i.e., the bacterial density at which the growth rate of the immune response is half its maximum. Bacteria grow and are killed by the innate immunity with a maximum killing rate ε. However, at high bacterial concentration bacteria can evade the immune response and reduce the immune killing efficiency (5, 16).
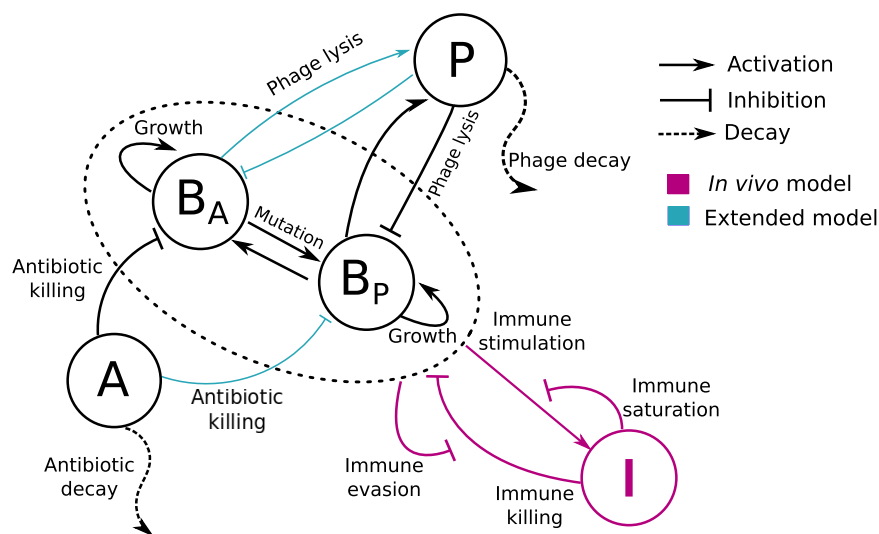
FIG 1 Schematic of the phage-antibiotic combination therapy model. Antibiotic-sensitive bacteria (B_A) and phage-sensitive bacteria (B_P) are targeted by antibiotic (A) and the phage (P), respectively. Host innate immune response interactions (pink arrows) are included in the *in vivo* model. Innate immunity (I) is activated by the presence of bacteria and attacks both bacterial strains. Furthermore, in model versions accounting for partial resistance (blue arrows), B_A and B_P are targeted by both antibiotic and phage but at quantitatively different levels.

Our model uses an implicit representation of spatial dynamics through different functional forms of phage-bacterium interactions [$F(P)$]. As such, we do not explicitly model the spatial dynamics of individual components. The model considers three modalities of phage infection, $F(P)$: linear, heterogeneous mixing (5, 22), and phage saturation (5). The linear phage infection modality assumes a well-mixed environment, where phage easily encounter and infect bacteria, so the infection rate $F(P) = \phi P$ is proportional to the phage density, where ϕ is the linear adsorption rate. The heterogeneous mixing model accounts for spatial heterogeneity, $F(P) = \Phi P^\gamma$, where Φ is the nonlinear adsorption rate and $\gamma < 1$ is the power-law exponent. The third modality assumes that at high phage density multiple phage particles adsorb to a single bacterium so that phage infection follows a saturating Hill function,

$$F(P) = \frac{\phi P}{1 + \dfrac{P}{P_C}}$$

Here, ϕ is the adsorption rate and P_C is the phage density at which the infection rate is half saturated.

Note that in later stages, we consider an "extended" combination therapy model (Fig. 1 [blue arrows]) in which bacterial strains are sensitive to both phage and antibiotic in quantitatively distinct levels. The full set of equations for this extension is found in the supplemental material. In addition, a full description of parameter choices is given in Materials and Methods.

RESULTS

Differential outcomes of single-phage therapy. We begin by exploring the dynamics arising from adding a single phage type at a density of 7.4×10^8 PFU/g 2 h after infections caused by either phage-sensitive or phage-resistant bacteria (Fig. 2). When the infection is caused by a phage-sensitive bacterium ($B_P = 7.4 \times 10^7$ CFU/g), phage lysis reduced B_P density to the point where the immune response alone could control this bacterial population. Despite the emergence of phage-resistant mutants (B_A), total bacterial population remained low and the innate immunity effectively controlled the infection. On the other hand, when the infection was caused by phage-resistant mutants ($B_A = 7.4 \times 10^7$ CFU/g), the phage could not target B_A, so the
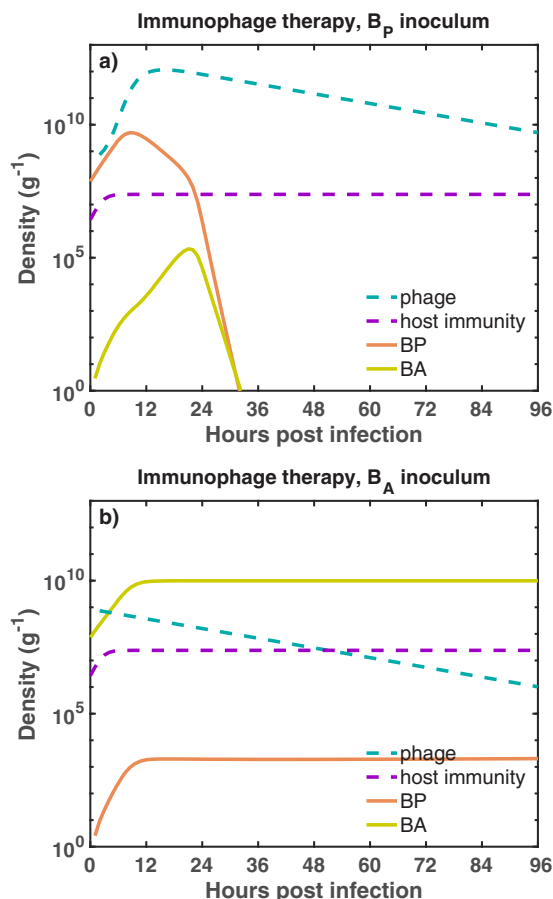
FIG 2 Dynamics of the immunophage therapy model against two different bacterial inocula. We simulate the phage therapy model developed in reference 16 against two infection settings. In the first infection setting (a), a phage-sensitive bacterial inoculum, B_P (orange solid line), is challenged with phage (blue dashed line) inside an immunocompetent host. In the second scenario (b), antibiotic-sensitive bacteria, B_A (green solid line), are challenged with phage in the presence of an active immune response (purple dashed line). The initial bacterial density and the initial phage density are $B_0 = 7.4 \times 10^7$ CFU/g and $P_0 = 7.4 \times 10^8$ PFU/g, respectively. For the simulation, we use a heterogeneous mixing model as a functional form of phage infection. The growth rates of B_P and B_A are $r_P = 0.75$ h^{-1} and $r_A = 0.67$ h^{-1}, respectively. Simulation run is 96 h with phage being administered 2 h after the infection. The bacterial carrying capacity is $K_C = 10^{10}$ CFU/g.

bacterial population grew unimpeded. The immune response was overwhelmed by the rapid growth of B_A, which then reached a density of ~10^{10} CFU/g after 12 h (Fig. 2b), leading to a persistent infection despite an activated immune response (similar to the outcomes described in reference 16).

This initial analysis illustrates how therapeutic outcomes given application of a single phage type may be strongly dependent on the initial bacterial inoculum. As expected, single-phage therapy fails to clear the infection when the bacterial inoculum is mistargeted (Fig. 2b). In the next section, we evaluate infection dynamics in response to the combined application of phage and antibiotics—similar to that in multiple *in vitro* and *in vivo* studies of phage-antibiotic treatment of MDR *P. aeruginosa* (7, 11).

Phage-antibiotic therapy treatment dynamics in immunocompetent hosts. We simulated the combined effects of phage (7.4×10^8 PFU/g) and antibiotics (assuming $2.5\times$ MIC of ciprofloxacin for the B_A strain) in two different infection settings. First, when an immunocompetent host was infected with phage-sensitive bacteria, the infection was cleared before ~36 h due to the combined killing effect of phage, antibiotic, and innate immunity. The dominant bacterial population, B_P, was targeted by the phage while the antibiotic targeted B_A. The combined effects of phage and

Phage-Antibiotic combination + Immune response
B_P inoculum, HM model

Phage-Antibiotic combination + Immune response
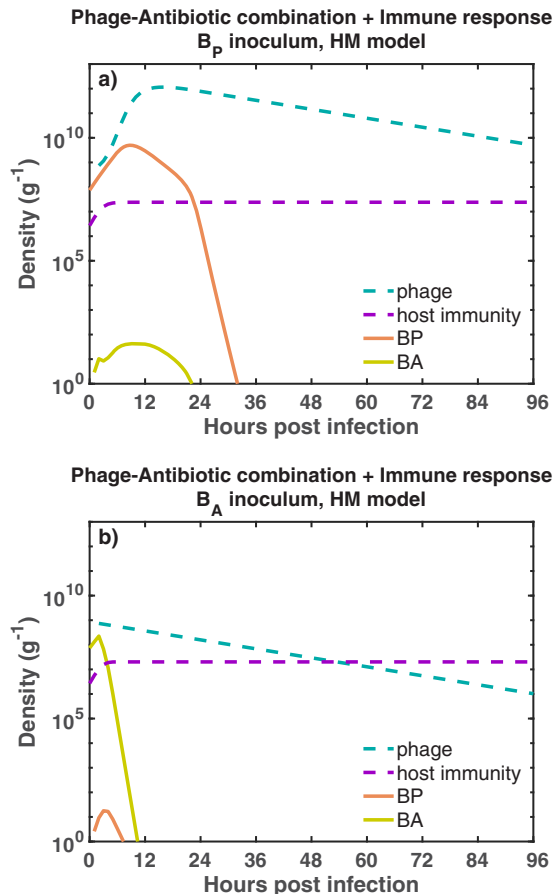**B_A inoculum, HM model**

FIG 3 Outcomes of the phage-antibiotic combination therapy model for two different infection settings. We simulate the combined effects of phage and antibiotics in an immunocompetent host infected with phage-sensitive bacteria (a), B_P (orange solid line). In panel b, the host is infected with antibiotic-sensitive bacteria, B_A (green solid line). The dynamics of the phage (blue dashed line) and innate immunity (purple dashed line) are shown for each infection setting. Initial bacterial density and phage density are $B_0 = 7.4 \times 10^7$ CFU/g and $P_0 = 7.4 \times 10^8$ PFU/g, respectively. For the simulation, we use a heterogeneous mixing model as a functional form of phage infection. The simulation run is 96 h (4 days). Antibiotic and phage are administered 2 h after the beginning infection. Ciprofloxacin is maintained at a constant concentration of 0.0350 μg/ml during the simulation. The carrying capacity of the bacteria is $K_C = 10^{10}$ CFU/g.

antibiotic reduced total bacterial density to the point where innate immunity eliminated the bacterial infection. Second, when the host was infected with antibiotic-sensitive bacteria, the pathogen was cleared (before ~12 h) due to the combined effect of phage, antibiotic, and innate immunity. The antibiotic facilitated the decrease of B_A while phage kept the B_P concentration low, easing the innate immunity control over the infection. The resulting infection clearance in the phage-resistant case (Fig. 3b) stands in stark contrast to the previous outcome of the single-phage therapy model (Fig. 2b). Overall, the results suggest that a curative outcome is possible when phage are combined with antibiotics in an immunocompetent host—even when the phage is initially mistargeted to the dominant bacterial strain. The results hold for different functional forms of phage-bacterium interactions $F(P)$ (see Fig. S1 in the supplemental material). However, what remains unclear is the extent to which successful treatment is driven by phage and antibiotics alone or, in part, because of the synergistic interactions with the innate immune response.

Phage-antibiotic combination therapy requires innate immunity to robustly clear the pathogen. In this section, we assess the dependency of combination therapy on the immune response. To do so, we evaluate the combination therapy while setting $I = 0$. This is meant to mimic conditions of severe immunodeficiency. In order to further
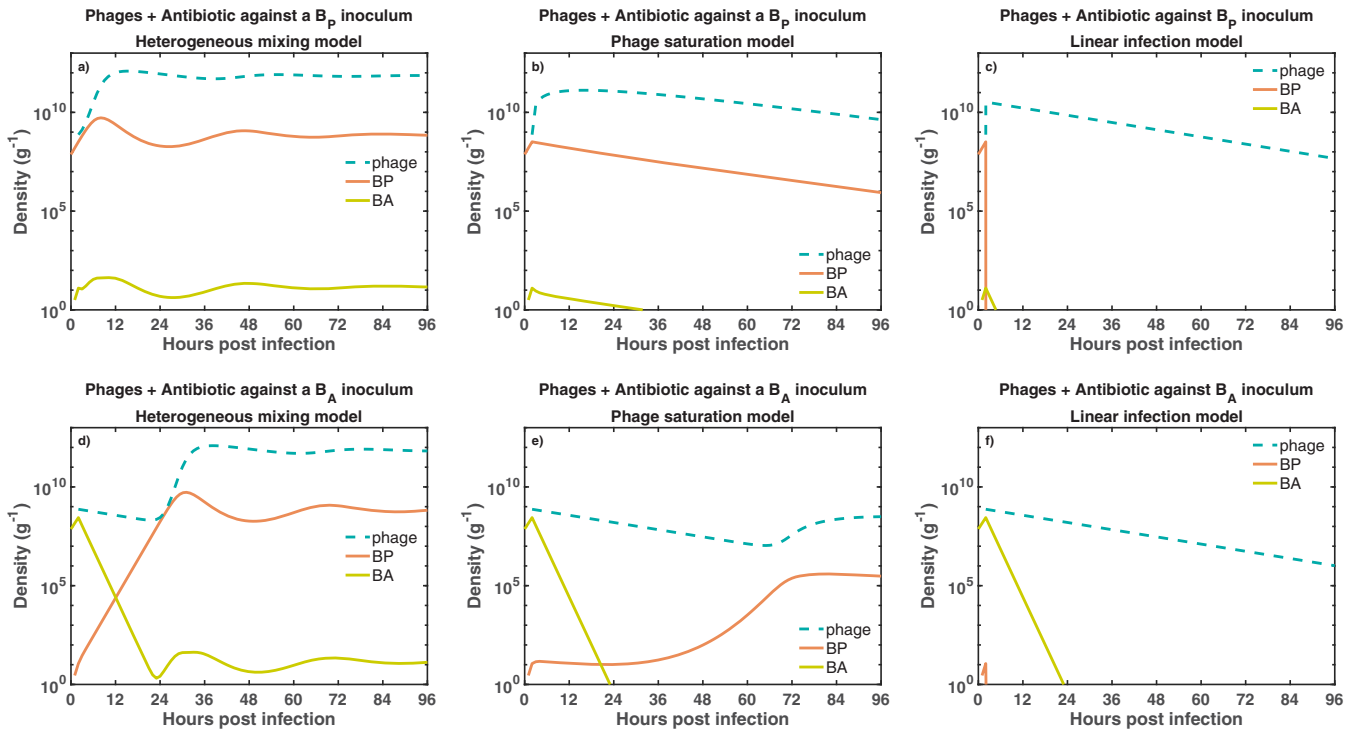
FIG 4 Bacterial dynamics given joint exposure to phage and antibiotic. We simulate bacterial growth for 96 h in exposure to phage (blue dashed line) and antibiotic (data not shown) added 2 h after the beginning of the inoculation. The combination of phage and antibiotic is tested against two different bacterial inocula. The first inoculum consisted of exclusively phage-sensitive bacteria (a to c), B_P (orange solid line). The second inoculum consisted of antibiotic-sensitive bacteria (d to f), B_A (green solid line). Additionally, we test three different models of phage infection, heterogeneous mixing (a and d), phage saturation (b and e), and linear infection (c and f). The initial bacterial density and phage density are $B_0 = 7.4 \times 10^7$ CFU/g and $P_0 = 7.4 \times 10^8$ PFU/g, respectively. Ciprofloxacin is maintained at a constant concentration of 2.5× MIC (i.e., 0.0350 μg/ml) during the simulations.

assess outcomes, we also consider multiple functional forms for phage-bacterium interactions—including the phage-saturation, heterogeneous mixing, and linear infection models (see Materials and Methods for more details).

First, when a phage-sensitive bacterial inoculum was challenged with the combination therapy, the pathogen persisted in two of three infection models. Bacteria persist in the heterogeneous mixing (HM) (Fig. 4a) and phage saturation (PS) (Fig. 4b) models, while the combination of phage and antibiotic successfully eliminates the bacterial population in the linear infection (LI) model (Fig. 4c). Although the combination of phage and antibiotic did not eliminate the bacterial population in the HM and PS models, the combination strategy still reduced the bacterial concentration relative to the carrying capacity ($K_C = 10^{10}$ CFU/g).

Second, when an antibiotic-sensitive bacterial inoculum was challenged with phage and antibiotic, bacteria persisted in two of three infection models, similarly to the previous phage-sensitive case. Bacteria persist in the HM (Fig. 4d) and PS (Fig. 4e) models, while bacterial population is eliminated in the LI model (Fig. 4f). Inclusion of antibiotics facilitated a decrease in B_A and the spread of B_P, leading to coexistence between bacteria and phage. Furthermore, the elimination of bacteria in the LI model took longer (~24 h) than in the previous phage-sensitive case.

The outcomes of the combination therapy model suggest that, in the absence of innate immunity, infection clearance is not achieved in two of three phage infection models. Pathogen clearance is achieved in only the linear infection case, that is, when we assume a well-mixed environment. On the other hand, when we assume spatial heterogeneity or phage saturation, a coexistence state between phage and bacteria arises from the tripartite dynamics between phage, bacteria, and antibiotic. Such a coexistence state is inconsistent with the expected antimicrobial effect of the combination therapy (7) and points to a potentially unrealized role of the immune response in the effectiveness of phage-antibiotic combination therapy.

TABLE 1 Summary of therapeutic outcomes given a combination of antibiotics (*A*), phage (*P*), and immunity (*I*)[a]

Treatment			Outcome
A	P	I	
1	0	0	Infection via B_P proliferation
1	0	1	Infection via B_P proliferation
1	1	0	Infection via B_P coexistence with phage
1	1	1	Curative

[a]The presence or absence of different antimicrobial agents is represented with 1 or 0, respectively.

Outcomes of the combination therapy model are robust to the bacterial composition of the inoculum and the concentration of antibiotic. Thus far, we have simulated two extreme infection inoculum scenarios involving exclusively phage-sensitive bacteria or exclusively antibiotic-sensitive bacteria. Next, we consider the effects of combination therapy on mixed bacterial inoculum containing both B_P and B_A. To do so, we performed a robustness analysis of four (*in silico*) therapy models, i.e., antibiotic-only, antibiotic-innate immunity, phage-antibiotic, and phage-antibiotic combination in the presence of innate immunity. For each model, we varied the concentration of the antibiotic and the bacterial composition of the inoculum. Outcomes from the different therapeutics are consistent with previous results obtained using a fixed set of initial conditions (Table 1). We find that model outcomes are robust to variations in the initial conditions (i.e., inoculum composition and concentration of ciprofloxacin).

First, we evaluated the killing effect of the antibiotic against mixed bacterial inoculum. We find that the pathogen persisted ($\sim 10^{10}$ CFU/g) for all different inoculum and concentrations of antibiotic. The antibiotic targeted B_A while B_P grew unimpeded in the absence of phage, such that B_P predominated after 96 h. In contrast, antibiotics and innate immunity (Fig. 5b) could eliminate bacterial inoculum with high percentages of antibiotic-sensitive bacteria (>90% of B_A). During this scenario, the low percentages of B_P coupled with the antibiotic killing of B_A facilitated the immune clearance of the infection. Furthermore, pathogen clearance was observed even for subinhibitory concentrations of ciprofloxacin. As is apparent, the antibiotic on its own cannot clear the infection, and therapeutic outcomes are only modestly improved in a narrow region of inoculum space.

Second, we assessed the effects of combining antibiotics with phage against mixed bacterial inoculum. The phage-antibiotic combination strategy failed to clear the infection for all combinations of initial conditions, consistent with the infection scenarios of the above section. Nonetheless, bacterial concentration was ~ 10 times smaller due to phage killing (orange area in Fig. 5c) than the bacterial concentration from the antibiotic-only therapy (bright yellow area of Fig. 5a). After 96 h of combined treatment, the phage-sensitive population was predominant at above MIC levels while antibiotic-sensitive bacteria populated the sub-MIC levels (Fig. S2 and S3 show the effects of different antibiotic levels on the bacterial dynamics). In contrast, a robust pathogen clearance was achieved when the phage-antibiotic combination strategy was supplemented with active innate immunity (Fig. 5d). Note that even partially effective immune responses can still be sufficient to achieve infection clearance (Fig. S4). Overall, the synergistic interactions between phage, antibiotic, and innate immunity led to clearance of the infection for the majority of initial conditions. The clearance region even spanned subinhibitory concentrations of ciprofloxacin.

We performed a further exploratory analysis of the combined therapy. We studied the effects of delay times on the application of the combined strategy, showing that therapeutic action is robust to delay times and fails irrespective of delay time when the immune system is compromised (Text S1; Fig. S5). We also performed a parameter sensitivity analysis (Text S1), showing that the combined strategy, when supplemented with the host immune response, is effective for a wide range of parameters (Fig. S6).
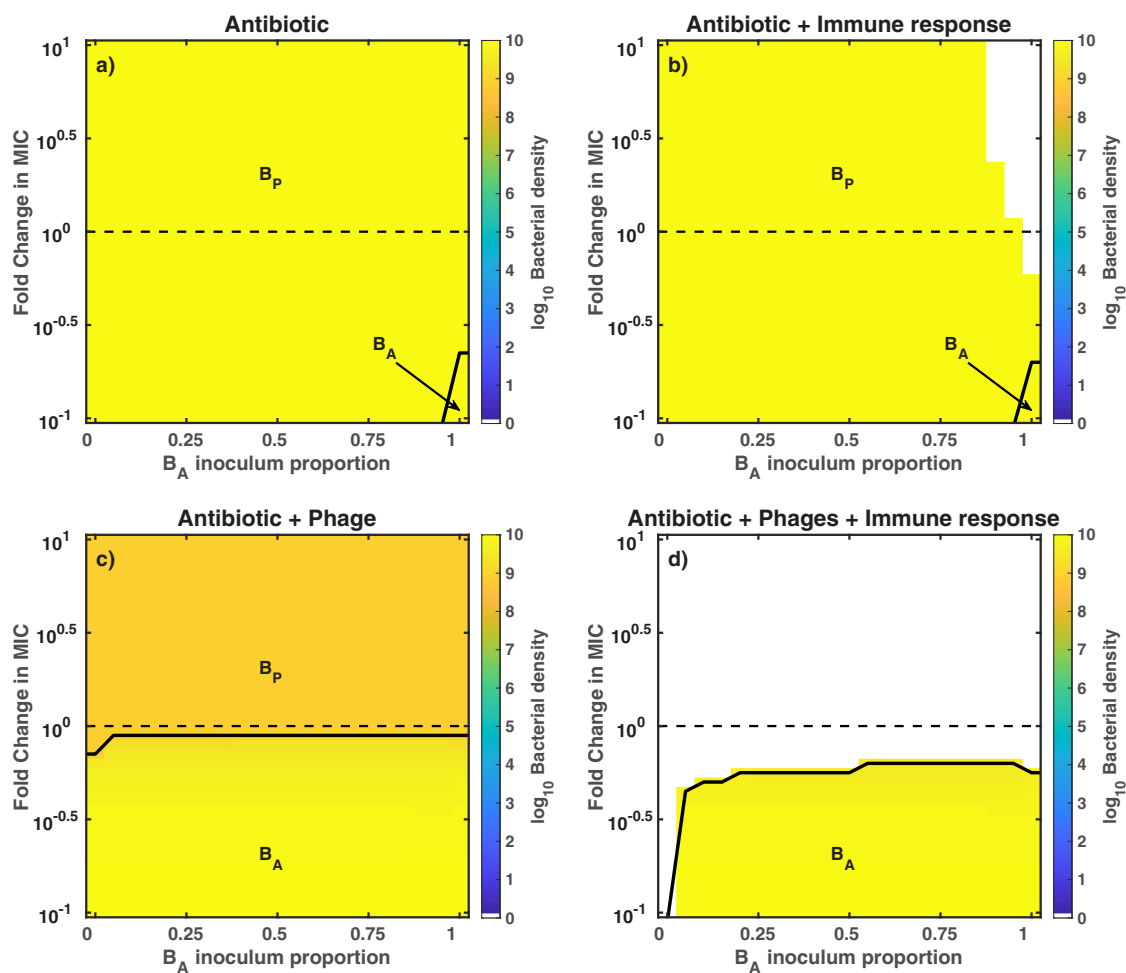
FIG 5 Outcomes of the robustness analysis for different antimicrobial strategies. We simulate the exposure of bacteria to different antimicrobial strategies, such as antibiotic-only (a), antibiotic plus innate immunity (b), phage plus antibiotic (c), and phage-antibiotic combination in the presence of innate immunity (d). The heatmaps show the bacterial density at 96 h postinfection. Colored regions represent bacterial persistence (e.g., orange areas for ~10^9 CFU/g and bright yellow areas for ~10^{10} CFU/g), while the white regions represent pathogen clearance. We vary the concentration of ciprofloxacin (MIC = 0.014 μg/ml), ranging from 0.1$\times$ MIC (0.0014 μg/ml) to 10$\times$ MIC (0.14 μg/ml), and the bacterial composition of the inoculum, ranging from 100% phage-sensitive bacteria (0% B_A) to 100% antibiotic-sensitive bacteria (100% B_A). Initial bacterial density and phage density (c and d) are $B_0 = 7.4 \times 10^7$ CFU/g and $P_0 = 7.4 \times 10^8$ PFU/g, respectively. Phage and antibiotic are administered 2 h after the beginning of the infection.

Finally, we note that these results derived from analysis of dynamics arising among extreme phenotypes. In reality, phage-sensitive strains may retain some sensitivity to antibiotics and antibiotic-sensitive strains can be infected at reduced levels by phage (7, 23, 24). Hence, we repeated the robustness analysis, using an extended model that incorporates quantitatively different levels of phage infectivity and antibiotic sensitivity of both strains (see Text S2). Partial resistance model outcomes are qualitatively consistent with previous outcomes of the extreme resistance model (contrast Fig. S7 with Fig. 5). Moreover, the bacterial dynamics of the partial resistance model are qualitatively similar to the dynamics arising among extreme phenotypes (contrast Fig. 3 with Fig. S8, bottom). Overall, our model analysis suggests that robust, curative success of phage-antibiotic combination therapy could be driven, in part, by a largely unrealized synergy with the immune response.

DISCUSSION

We have developed a combination therapy model that combines phage and antibiotics against a mixed-strain infection of *Pseudomonas aeruginosa*. The model suggests that infection clearance arises from nonlinear synergistic interactions between

phage, antibiotic, and innate immunity. Moreover, the infection clearance shows robustness to variations in the concentration of antibiotic, delays in the administration of the combined therapy, the bacterial composition of the inoculum, and model assumptions. In contrast, when innate immunity responses are removed (or severely reduced), then phage-antibiotic combination therapy is predicted to fail to eliminate the infection. This suggests that combined therapy may depend critically on immune response for resolving bacterial infections.

The *in silico* findings are consistent with qualitative, experimental outcomes *in vitro* and *in vivo*. For example, one of our main results states that phage-antibiotic combined therapy has a greater antimicrobial effect than single-phage or antibiotic therapies; this is consistent with several *in vitro* settings that show a greater bacterial density reduction for combined rather than single therapies (25–28). Moreover, additional studies explore the use of sublethal concentrations of antibiotics otherwise insufficient for controlling bacterial growth but efficient when combined with phage against diverse bacterial populations (25, 26, 28, 29). These findings are consistent with our *in silico* outcomes where pathogen clearance is observed at sub-MIC antibiotic levels in the combined therapy framework. Further work to compare model-based predictions to experiments will require moving beyond outcomes to high-resolution temporal data.

In connecting models to experiment, it is important to consider extending the model framework to a spatially explicit context. Spatial structure can be relevant therapeutically. For example, during chronic infections spatially organized bacterial aggregates of *P. aeruginosa* protect themselves against phage killing by producing exopolysaccharides (30). Furthermore, modeling efforts have shown that spatial structure affects the therapeutic success of phage therapy (31) and phage-antibiotic combination therapy (32). For example, structured environments limit phage dispersion and amplification, promoting bacterial survival and resistance acquisition (31, 32). Moreover, the heterogeneous distribution of antibiotic creates spatial refuges (of low or null antimicrobial presence) where bacteria survive and resistant mutants arise (32). The current model also neglects the complex features of immune response termination (33) and interactions with commensal microbes (34), both priority areas for future work.

In conclusion, the phage-antibiotic combination therapy model developed here describes efforts to explore how host immunity modulates infection outcomes. As we have shown, immune clearance of pathogens may lie at the core of the curative success of combination treatments. If so, this additional synergy may help to resolve the resistance problem and also guide use of sub-MICs of antibiotics. Besides reducing toxic side effects associated with high concentrations of antibiotics, sub-MICs can improve phage infectivity through morphological changes of the bacterial cell (9, 35, 36) or by not interfering with the phage replication cycle (25, 26). When combined in an immunocompetent context, we find that phage-antibiotic combination therapy is robust to quantitatively and qualitatively distinct resistance profiles. These findings reinforce findings that phage and antibiotics can be used to treat a certain class of MDR *P. aeruginosa* pathogens in patients (11, 37). Model results also highlight the role of the immune response in realizing curative success—which will be relevant to expanding combination theory for a range of clinical applications.

MATERIALS AND METHODS

Model simulation. The numerical integration of the combination therapy model is carried out using ODE45 in Matlab. We obtain the temporal dynamics of two bacterial strains, phage, antibiotic, and innate immune response. Moreover, we set an extinction threshold of 1 g^{-1}; hence, when B_P or B_A densities are ≤1 CFU/g at any time during the simulation, we set their densities to 0 CFU/g. We run all the simulations for 96 h (4 days).

Robustness analysis. We perform a robustness analysis of the phage-antibiotic combination therapy model by varying its initial conditions. We vary the concentration of antibiotic from sub-MICs (0.1× MIC) to above MICs (10× MIC), using the MIC of ciprofloxacin (0.014 μg/ml) for the PAPS phage-resistant strain as a reference (11). Moreover, we vary the bacterial composition of the inoculum by increasing the bacterial

TABLE 2 Microbiology and phage-associated parameter values

Parameter of model	Value	Source from which estimated
Combination therapy model		
r_P, maximum growth rate of phage-sensitive (antibiotic-resistant) bacteria	0.75 h^{-1}	*P. aeruginosa* murine pneumonia model (40)
K_C, carrying capacity of bacteria	1×10^{10} CFU/g	Assuming ~4 times above the typical bacterial density (2.4×10^9 CFU/g) in wild-type mice 24 h postinfection
β, burst size of phage	100	Estimated from reference 5
ω, decay rate of phage	0.07 h^{-1}	Estimated from reference 5
ε, killing rate parameter of immune response	8.2×10^{-8} g/(h cell)	Set such that εK_I gives the maximum granulocyte killing rate (40)
α, maximum growth rate of immune response	0.97 h^{-1}	Fitting of neutrophil recruitment data (41)
K_I, maximum capacity of immune response	2.4×10^7 cell/g	Fitting of neutrophil recruitment data (41)
K_I, maximum capacity of immune response (immunodeficient mice)	Same as I_0	No innate immune activation
K_D, bacterial concentration at which immune response is half as effective	4.1×10^7 CFU/g	Corresponds to lethal dose of about 5.5×10^6 CFU/lungs
K_N, bacterial concentration when immune response growth rate is half its maximum	10^7 CFU/g	*In vitro* data of TLR5 response to PAK strain (42)
B_0, initial bacterial density (in presence or absence of the innate immune response)	7.4×10^7 CFU/g	Total inoculum of 10^7 CFU
P_0, initial phage dose (in presence or absence of the innate immune response)	7.4×10^8 PFU/g	Total phage dose of 10^8 PFU
I_0, initial immune response	2.7×10^6 cell/g	Fitting of neutrophil recruitment data (41)
I_0, initial immune response (immunodeficient mice)	0 cell/g	Assuming no primary innate immunity
HM model		
$\bar{\phi}$, nonlinear phage adsorption rate	5.4×10^{-8} (g/PFU)$^\gamma$ h^{-1}	Estimated from reference 5
γ, power law exponent in phage infection rate	0.6	Estimated from reference 5
PS model		
ϕ, linear phage adsorption rate	5.4×10^{-8} (g/PFU) h^{-1}	Estimated from reference 5
P_C, phage concentration at which phage infection rate is half saturated	1.5×10^7 PFU/g	Estimated from reference 5
LI model		
ϕ, linear phage adsorption rate	5.4×10^{-8} (g/PFU) h^{-1}	Estimated from reference 5

density of one strain (e.g., B_A) by 5% and decreasing the density of the other by 5%. Then, we select a pair of initial conditions and run the model 96 h. Finally, we calculate total bacterial density, $B_{total} = B_A + B_P$.

Parameter estimation. The parameter values used in the simulations of the combination therapy model are shown in Tables 2 and 3. Most of the parameter estimation was carried out in previous work (see "Parameter Estimation" section in reference 5), supplemented by parameters associated with functions describing the pharmacodynamics and pharmacokinetics of ciprofloxacin (18, 38).

TABLE 3 Additional parameter values associated with the effects of antibiotics

Antibiotic (ciprofloxacin) parameter	Value	How calculated
κ_{kill}, maximum antibiotic killing rate	18.5 h^{-1}	Fitting an E_{max} model to antibiotic kill curves (18)
EC_{50}, concentration of antibiotic at which the killing rate is half its maximum	0.3697 μg/ml	Calculated using the MIC of ciprofloxacin for the phage-resistant PAPS strain (7)
EC_{B_P}, concentration of antibiotic at which the killing rate is half its maximum	4.070 μg/ml	Calculated using the MIC of ciprofloxacin for the phage-sensitive PAPS strain (7)
H, Hill coefficient	1	From reference 18
MIC of ciprofloxacin for *P. aeruginosa* PAPS phage-resistant strain	0.014 μg/ml	From reference 7
MIC of ciprofloxacin for *P. aeruginosa* PAPS phage-sensitive strain	0.172 μg/ml	From reference 7
θ, antibiotic elimination rate from serum samples	0.53 h^{-1}	Estimated from antibiotic concentration-vs-time curves; concentration of ciprofloxacin was measured in serum samples of *P. aeruginosa*-infected mice (38)
Antibiotic-sensitive bacterial parameters		
μ_1, probability of emergence of antibiotic-sensitive (phage-resistant) mutants per cellular division	2.85×10^{-8}	Estimated from experimental measurements (39)
μ_2, probability of emergence of phage-sensitive (antibiotic-resistant) mutants per cellular division	2.85×10^{-8}	Approximated to the estimates from reference 39
r_A, maximum growth rate of antibiotic-sensitive (phage-resistant) bacteria	0.675 h^{-1}	10% tradeoff between resistance against phage and growth rate (43)

TABLE 4 Phage adsorption rate of phage-sensitive and phage-resistant *Pseudomonas aeruginosa* strains

Phage adsorption rate (%) for strain type:			
Phage sensitive	Phage resistant	Fold decrease	Reference
31.3	9.6	3.2	23
73.7	66.5–2.4	~1.1 to ~30	44
87.2	42.8	2	44
92.7	55.3 and 42.8	1.6 and 2	24

The pharmacodynamics of ciprofloxacin (CP) is described by the following maximum effect (E_{max}) model (18):

$$\kappa_{kill} \frac{A^H}{EC_{50}^H + A^H}.$$

where κ_{kill} represents the maximum killing rate of the antibiotic, EC_{50} is the antibiotic concentration at which the antibiotic killing rate is half its maximum, and H is a Hill coefficient. The values of the parameters are obtained using *in vitro* growth curves of *P. aeruginosa* at different concentrations of CP (18). The elimination rate of the antibiotic, θ, is estimated from levels of clearance of CP from serum samples of mice infected with *P. aeruginosa* (38). The EC_{50} parameter value is adjusted in our model to consider the MIC of CP for the PAPS reference strain (7).

The probabilities of producing a mutant strain per cell division, μ_1 and μ_2, are obtained from reference 39, where μ_1 is the probability of producing a phage-resistant (antibiotic sensitive) mutant per cell division and μ_2 is the probability of generating a phage-sensitive (antibiotic-resistant) mutant per cell division.

To account for partially resistant strains, we extend our combination therapy model (Text S2, equations S21 to S25) and include the parameters EC_{B_P} and δ_P. EC_{B_P} is the half-saturation constant of the antibiotic killing function and modulates the level of antibiotic resistance for B_P. The parameter was calculated based on the MIC of CP for the PAPS phage-sensitive strain (7). Moreover, for modulating the level of resistance to phage infection [$F(P)$] of B_A, we use the parameter $\delta_P < 1$ (Table 4).

Data availability. The code used to simulate the phage-antibiotic combination therapy model and generate the main figures as well as the supplemental material figures can be found in the GitHub repository at https://github.com/WeitzGroup/phage_antibiotic.

SUPPLEMENTAL MATERIAL

Supplemental material is available online only.
TEXT S1, PDF file, 0.1 MB.
TEXT S2, PDF file, 0.1 MB.
FIG S1, PDF file, 0.1 MB.
FIG S2, PDF file, 0.1 MB.
FIG S3, PDF file, 0.03 MB.
FIG S4, PDF file, 0.02 MB.
FIG S5, PDF file, 0.1 MB.
FIG S6, PDF file, 0.1 MB.
FIG S7, PDF file, 0.04 MB.
FIG S8, PDF file, 0.04 MB.

REFERENCES

1. World Health Organization. 2017. Antibacterial agents in clinical development: an analysis of the antibacterial clinical development pipeline, including tuberculosis. Technical report WHO/EMP/IAU/2017.12. World Health Organization, Geneva, Switzerland.
2. Centers for Disease Control and Prevention. 2013. Antibiotic resistance threats in the United States, 2013. Technical report. Centers for Disease Control and Prevention, US Department of Health and Human Services, Atlanta, GA.
3. European Centre for Disease Prevention and Control and European Medicines Agency. 2009. The bacterial challenge: time to react. Technical report EMEA/576176/2009. European Centre for Disease Prevention and Control/European Medicines Agency, Solna, Sweden.
4. Oechslin F, Piccardi P, Mancini S, Gabard J, Moreillon P, Entenza JM, Resch G, Que Y-A. 2017. Synergistic interaction between phage therapy and antibiotics clears *Pseudomonas aeruginosa* infection in endocarditis and reduces virulence. J Infect Dis 215:703–712. https://doi.org/10.1093/infdis/jiw632.
5. Roach DR, Leung CY, Henry M, Morello E, Singh D, Santo JPD, Weitz JS, Debarbieux L. 2017. Synergy between the host immune system and bacteriophage is essential for successful phage therapy against an acute respiratory pathogen. Cell Host Microbe 22:38–47. https://doi.org/10.1016/j.chom.2017.06.018.
6. Torres-Barceló C, Franzon B, Vasse M, Hochberg ME. 2016. Long-term

effects of single and combined introductions of antibiotics and bacteriophages on populations of *Pseudomonas aeruginosa*. Evol Appl 9:583–595. https://doi.org/10.1111/eva.12364.

7. Chan BK, Sistrom M, Wertz JE, Kortright KE, Narayan D, Turner PE. 2016. Phage selection restores antibiotic sensitivity in MDR *Pseudomonas aeruginosa*. Sci Rep 6:26717. https://doi.org/10.1038/srep26717.

8. Stern A, Sorek R. 2011. The phage-host arms race: shaping the evolution of microbes. Bioessays 33:43–51. https://doi.org/10.1002/bies.201000071.

9. Knezevic P, Curcin S, Aleksic V, Petrusic M, Vlaski L. 2013. Phage-antibiotic synergism: a possible approach to combatting *Pseudomonas aeruginosa*. Res Microbiol 164:55–60. https://doi.org/10.1016/j.resmic.2012.08.008.

10. Schooley RT, Biswas B, Gill JJ, Hernandez-Morales A, Lancaster J, Lessor L, Barr JJ, Reed SL, Rohwer F, Benler S, Segall AM, Taplitz R, Smith DM, Kerr K, Kumaraswamy M, Nizet V, Lin L, McCauley MD, Strathdee SA, Benson CA, Pope RK, Leroux BM, Picel AC, Mateczun AJ, Cilwa KE, Regeimbal JM, Estrella LA, Wolfe DM, Henry MS, Quinones J, Salka S, Bishop-Lilly KA, Young R, Hamilton T. 2017. Development and use of personalized bacteriophage-based therapeutic cocktails to treat a patient with a disseminated resistant *Acinetobacter baumannii* infection. Antimicrob Agents Chemother 61: e00954-17. https://doi.org/10.1128/AAC.00954-17.

11. Chan BK, Turner PE, Kim S, Mojibian HR, Elefteriades JA, Narayan D. 2018. Phage treatment of an aortic graft infected with *Pseudomonas aeruginosa*. Evol Med Public Health 2018:60–66. https://doi.org/10.1093/emph/eoy005.

12. Burmeister AR, Bender RG, Fortier A, Lessing AJ, Chan BK, Turner PE. 2018. Two lytic bacteriophages that depend on the *Escherichia coli* multi-drug efflux gene tolC and differentially affect bacterial growth and selection. bioRxiv 397695. https://doi.org/10.1101/397695.

13. German GJ, Misra R. 2001. The TolC protein of Escherichia coli serves as a cell-surface receptor for the newly characterized TLS bacteriophage. J Mol Biol 308:579–585. https://doi.org/10.1006/jmbi.2001.4578.

14. Ricci V, Piddock LJ. 2010. Exploiting the role of TolC in pathogenicity: identification of a bacteriophage for eradication of Salmonella serovars from poultry. Appl Environ Microbiol 76:1704–1706. https://doi.org/10.1128/AEM.02681-09.

15. Fan F, Li X, Pang B, Zhang C, Li Z, Zhang L, Li J, Zhang J, Yan M, Liang W, Kan B. 2018. The outer-membrane protein TolC of Vibrio cholerae serves as a second cell-surface receptor for the VP3 phage. J Biol Chem 293:4000–4013. https://doi.org/10.1074/jbc.M117.805689.

16. Leung C, Weitz JS. 2017. Modeling the synergistic elimination of bacteria by phage and the innate immune system. J Theor Biol 429:241–252. https://doi.org/10.1016/j.jtbi.2017.06.037.

17. Cairns BJ, Timms AR, Jansen VAA, Connerton IF, Payne RJH. 2009. Quantitative models of in vitro bacteriophage-host dynamics and their application to phage therapy. PLoS Pathog 5:e1000253. https://doi.org/10.1371/journal.ppat.1000253.

18. Delacher S, Derendorf H, Hollenstein U, Brunner M, Joukhadar C, Hofmann S, Georgopoulos A, Eichler HG, Müller M. 2000. A combined in vivo pharmacokinetic-in vitro pharmacodynamic approach to simulate target site pharmacodynamics of antibiotics in humans. J Antimicrob Chemother 46:733–739. https://doi.org/10.1093/jac/46.5.733.

19. Regoes RR, Wiuff C, Zappala RM, Garner KN, Baquero F, Levin BR. 2004. Pharmacodynamic functions: a multiparameter approach to the design of antibiotic treatment regimens. Antimicrob Agents Chemother 48: 3670–3676. https://doi.org/10.1128/AAC.48.10.3670-3676.2004.

20. Wen X, Gehring R, Stallbaumer A, Riviere JE, Volkova VV. 2016. Limitations of MIC as sole metric of pharmacodynamic response across the range of antimicrobial susceptibilities within a single bacterial species. Sci Rep 6:37907. https://doi.org/10.1038/srep37907.

21. Salahudeen MS, Nishtala PS. 2017. An overview of pharmacodynamic modelling, ligand-binding approach and its application in clinical practice. Saudi Pharm J 25:165–175. https://doi.org/10.1016/j.jsps.2016.07.002.

22. Roy M, Pascual M. 2006. On representing network heterogeneities in the incidence rate of simple epidemic models. Ecol Complex 3:80–90. https://doi.org/10.1016/j.ecocom.2005.09.001.

23. Chibeu A, Ceyssens P-J, Hertveldt K, Volckaert G, Cornelis P, Matthijs S, Lavigne R. 2009. The adsorption of Pseudomonas aeruginosa bacteriophage phiKMV is dependent on expression regulation of type IV pili genes. FEMS Microbiol Lett 296:210–218. https://doi.org/10.1111/j.1574-6968.2009.01640.x.

24. Cui X, You J, Sun L, Yang X, Zhang T, Huang K, Pan X, Zhang F, He Y, Yang H. 2016. Characterization of *Pseudomonas aeruginosa* phage C11 and identification of host genes required for virion maturation. Sci Rep 6:39130. https://doi.org/10.1038/srep39130.

25. Chaudhry WN, Concepcion-Acevedo J, Park T, Andleeb S, Bull JJ, Levin BR. 2017. Synergy and order effects of antibiotics and phages in killing

Pseudomonas aeruginosa biofilms. PLoS One 12:e0168615. https://doi.org/10.1371/journal.pone.0168615.

26. Akturk E, Oliveira H, Santos SB, Costa S, Kuyumcu S, Melo LD, Azeredo J. 2019. Synergistic action of phage and antibiotics: parameters to enhance the killing efficacy against mono and dual-species biofilms. Antibiotics 8:103. https://doi.org/10.3390/antibiotics8030103.

27. Henriksen K, Rørbo N, Rybtke ML, Martinet MG, Tolker-Nielsen T, Høiby N, Middelboe M, Ciofu O. 2019. *P aeruginosa* flow-cell biofilms are enhanced by repeated phage treatments but can be eradicated by phage-ciprofloxacin combination: monitoring the phage-*P. aeruginosa* biofilms interactions. Pathog Dis 77:ftz011. https://doi.org/10.1093/femspd/ftz011.

28. Dickey J, Perrot V. 2019. Adjunct phage treatment enhances the effectiveness of low antibiotic concentration against *Staphylococcus aureus* biofilms in vitro. PLoS One 14:e0209390. https://doi.org/10.1371/journal.pone.0209390.

29. Lin Y, Chang RYK, Britton WJ, Morales S, Kutter E, Chan H-K. 2018. Synergy of nebulized phage PEV20 and ciprofloxacin combination against *Pseudomonas aeruginosa*. Int J Pharm 551:158–165. https://doi.org/10.1016/j.ijpharm.2018.09.024.

30. Darch SE, Kragh KN, Abbott EA, Bjarnsholt T, Bull JJ, Whiteley M. 2017. Phage inhibit pathogen dissemination by targeting bacterial migrants in a chronic infection model. mBio 8:e00240-17. https://doi.org/10.1128/mBio.00240-17.

31. Bull J, Christensen K, Scott C, Jack B, Crandall C, Krone S. 2018. Phage-bacterial dynamics with spatial structure: self organization around phage sinks can promote increased cell densities. Antibiotics 7:8. https://doi.org/10.3390/antibiotics7010008.

32. de Sousa JAM, Rocha EP. 2019. Environmental structure drives resistance to phages and antibiotics during phage therapy and to invading lysogens during colonisation. Sci Rep 9:3149. https://doi.org/10.1038/s41598-019-39773-3.

33. Boone DL, Turer EE, Lee EG, Ahmad R-C, Wheeler MT, Tsui C, Hurley P, Chien M, Chai S, Hitotsumatsu O, McNally E, Pickart C, Ma A. 2004. The ubiquitin-modifying enzyme A20 is required for termination of Toll-like receptor responses. Nat Immunol 5:1052–1060. https://doi.org/10.1038/ni1110.

34. Leung C-Y, Weitz JS. 2019. Not by (good) microbes alone: towards immunocommensal therapies. Trends Microbiol 27:294–302. https://doi.org/10.1016/j.tim.2018.12.006.

35. Comeau AM, Tétart F, Trojet SN, Prere M-F, Krisch H. 2007. Phage-antibiotic synergy (PAS): β-lactam and quinolone antibiotics stimulate virulent phage growth. PLoS One 2:e799. https://doi.org/10.1371/journal.pone.0000799.

36. Kaur S, Harjai K, Chhibber S. 2012. Methicillin-resistant *Staphylococcus aureus* phage plaque size enhancement using sublethal concentrations of antibiotics. Appl Environ Microbiol 78:8227–8233. https://doi.org/10.1128/AEM.02371-12.

37. McCallin S, Sacher JC, Zheng J, Chan BK. 2019. Current state of compassionate phage therapy. Viruses 11:343. https://doi.org/10.3390/v11040343.

38. Macia MD, Borrell N, Segura M, Gomez C, Perez JL, Oliver A. 2006. Efficacy and potential for resistance selection of antipseudomonal treatments in a mouse model of lung infection by hypermutable *Pseudomonas aeruginosa*. Antimicrob Agents Chemother 50:975–983. https://doi.org/10.1128/AAC.50.3.975-983.2006.

39. Luria SE, Delbrück M. 1943. Mutations of bacteria from virus sensitivity to virus resistance. Genetics 28:491–511.

40. Drusano G, Vanscoy B, Liu W, Fikes S, Brown D, Louie A. 2011. Saturability of granulocyte kill of *Pseudomonas aeruginosa* in a murine model of pneumonia. Antimicrob Agents Chemother 55:2693–2695. https://doi.org/10.1128/AAC.01687-10.

41. Reutershan J, Basit A, Galkina EV, Ley K. 2005. Sequential recruitment of neutrophils into lung and bronchoalveolar lavage fluid in LPS-induced acute lung injury. Am J Physiol Lung Cell Mol Physiol 289:L807–L815. https://doi.org/10.1152/ajplung.00477.2004.

42. Zhang Z, Louboutin J-P, Weiner DJ, Goldberg JB, Wilson JM. 2005. Human airway epithelial cells sense *Pseudomonas aeruginosa* infection via recognition of flagellin by Toll-like receptor 5. Infect Immun 73: 7151–7160. https://doi.org/10.1128/IAI.73.11.7151-7160.2005.

43. Bohannan BJ, Kerr B, Jessup CM, Hughes JB, Sandvik G. 2002. Trade-offs and coexistence in microbial microcosms. Antonie Van Leeuwenhoek 81:107–115. https://doi.org/10.1023/A:1020585711378.

44. Roncero C, Darzins A, Casadaban M. 1990. *Pseudomonas aeruginosa* transposable bacteriophages D3112 and B3 require pili and surface growth for adsorption. J Bacteriol 172:1899–1904. https://doi.org/10.1128/JB.172.4.1899-1904.1990.